AIMS Biophysics

http://www.aimspress.com/journal/biophysics/

AIMS Biophysics, 8(2): 182–197.
DOI: 10.3934/biophy.2021014
Received: 03 March 2021
Accepted: 20 April 2021
Published: 22 April 2021

Research article

Dynamical analysis of fractional-order chemostat model

Nor Afiqah Mohd Aris and Siti Suhana Jamaian*

Department of Mathematics and Statistics, Faculty of Applied Sciences and Technology, Universiti Tun Hussein Onn Malaysia, Pagoh Education Hub, 84600 Pagoh, Johor, Malaysia

* **Correspondence:** Email: suhana@uthm.edu.my; Tel: +60197970079.

Abstract: The fractional-order differential equations is studied to describe the dynamic behaviour of a chemostat system. The integer-order chemostat model in the form of the ordinary differential equation is extended to the fractional-order differential equations. The stability and bifurcation analyses of the fractional-order chemostat model are investigated using the Adams-type predictor-corrector method. The result shows that increasing or decreasing the value of the fractional order, α, may stabilise the unstable state of a chemostat system and also may destabilised the stable state of the chemostat system depend on the predefined parameter values. The increasing the value of the initial substrate concentration, S_0 may destabilise the stable state of a chemostat system and stabilise the unstable state of the system. Therefore, the running state of a fractional-order chemostat system is affected by the value of α and the value of the initial substrate concentration, S_0. In actual application, the value of the initial substrate should remain at $S_0 \geq 2.54$ to ensure that the chemostat system is unstable state. There will be some change in the amount of the cell mass concentration whether increase or decrease when the system is unstable. Therefore, the chemostat system can be well-controlled for the production of cell mass.

Keywords: fractional-order differential equation; chemostat model; Adams-type predictor corrector method; Hopf bifurcation; Monod expression

1. Introduction

Numerous mathematical models have been established to predict and study the biological system. In the past four decades, there have been far-reaching research on improving cell mass production in chemical reactors [1]. The chemostat model is used to understand the mechanism of cell mass growth in a chemostat. A chemostat is an apparatus for continuous culture that contains bacterial populations. It can be used to investigate the cell mass production under controlled conditions. This reactor provides a dynamic system for population studies and is suitable to be used in a laboratory. A

substrate is continuously added into the reactor containing the cell mass, which grows by consuming the substrate that enters through the inflow chamber. Meanwhile, the mixture of cell mass and substrate is continuously harvested from the reactor through the outflow chamber. The dynamics in the chemostat can be investigated by using the chemostat model [2].

Ordinary differential equations (ODEs) are commonly used for modelling biological systems. However, most biological systems behaviour has memory effects, and ODEs usually neglect such effects. The fractional-order differential equations (FDEs) are taken into account when describing the behaviour of the systems' equations. A FDEs is a generalisation of the ODEs to random nonlinear order [3]. This equation is more effective because of its good memory, among other advantages [4–8]. The errors occuring from the disregarded parameters when modelling of phenomena in real-life also can be reduced. FDEs are also used to efficiently replicate the real nature of various systems in the field of engineering and sciences [9]. In the past few decades, FDEs have been used in biological systems for various studies [5, 6, 10–17].

Since great strides in the study of FDEs have been developed, the dynamics in the chemostat can be investigated using the mathematical model of the chemostat in the form of FDEs. Moreover, there have been few studies on the expansion of the chemostat model with fractional-order theory. Thus, we deepen and complete the analysis on the integer-order chemostat model with fractional-order theory and discuss the stability of the equilibrium points of the fractional-order chemostat model. Next, the bifurcation analysis for the fractional-order chemostat model is conducted to identify the bifurcation point that can change the stability of the system. The analysis identifies the values of the fractional-order and the system parameters to ensure the operation of the chemostat is well-controlled.

2. Materials and methods

2.1. Definition of Caputo derivative

Recently, there are many approaches to define fractional operators such as by Caputo, Riemann-Liouville, Hadamard, and Grunwald-Letnikov [3]. However, Caputo is often used due to its convenience in various applications [18]. Caputo is also useful to encounter an obstacle where the initial condition is done in the differential of integer-order [19]. In this paper, we applied Caputo derivative to define the system of fractional-order. The Caputo derivative for the left-hand side is defined as

$$D_t^{\alpha} f(t) = \frac{1}{\Gamma(n-\alpha)} \int_0^t \frac{f^{(n)}\tau}{(t-\tau)^{\alpha-n+1}} d\tau, \tag{2.1}$$

where Γ denotes the function of gamma, n is an integer, where $n-1 < \alpha < n$ [18].

2.2. Adams-type predictor corrector method

The Adams-type predictor-corrector method is one of the technique that have been proposed for fractional-order differential equations [19–21]. The Adams-type predictor-corrector method is a analysis of numerical algorithm that involves two basics steps: predictor and corrector. The predictor

formula can be described as

$$y_h^P(t_{n+1}) = \sum_{k=0}^{\lceil\alpha\rceil-1} \frac{t_{n+1}^k}{k!} y_0^{(k)} + \frac{1}{\Gamma(\alpha)} \sum_{j=0}^{n} b_{j,n+1} f\left(t_j, y_h\left(t_j\right)\right), \tag{2.2}$$

meanwhile the corrector formula can be determined by

$$y_h(t_{n+1}) = \sum_{k=0}^{\lceil\alpha\rceil-1} \frac{t_{n+1}^k}{k!} + \frac{h^\alpha}{\Gamma(\alpha+2)} f\left(t_{n+1}, y_h^P(t_{n+1})\right) + \frac{h^\alpha}{\Gamma(\alpha+2)} \sum_{j=0}^{n} f\left(t_j, y_h\left(t_j\right)\right). \tag{2.3}$$

The predictor-corrector method is also called as the PECE (Predict, Evaluate, Correct, Evaluate) method [22]. The procedure of the predictor-corrector method can be explained as follows

(i) Calculate the predictor step, $y_h^P(t_{n+1})$ in Eq. (2.2).

(ii) Evaluate $f\left(t_{n+1}, y_h^P(t_{n+1})\right)$.

(iii) Calculate the corrector step, $y_h(t_{n+1})$ in Eq. (2.3).

(iv) Evaluate $f(t_{n+1}, y_h(t_{n+1}))$.

The procedure repeatedly predicts and corrects the value until the corrected value becomes a converged number [21]. This method is able to maintain the stability of the properties and has good accuracy. Moreover, this method also has lower computational cost than other methods [23]. The algorithm of the Adams-type predictor-corrector method proposed by [22] is shown in Appendix.

2.3. Stability analysis of fractional-order system

The conditions of stability for integer-order differential equations and fractional-order differential equations are different. Both systems could have the same steady-state points but different stability conditions [24, 25]. The stability condition for fractional-order differential equations can be stated by Theorem 1 and the Routh-Hurwitz stability condition as described by Proposition 1.

Theorem 1 [5, 6, 26]. The commensurate system of fractional-order where $x \in \mathbb{R}$ and $0 < \alpha < 1$ is locally asymptotically stable if the eigenvalues of the Jacobian matrix evaluated at the steady-state point is satisfied by

$$|arg(\lambda)| > \frac{\alpha\pi}{2}. \tag{2.4}$$

Proposition 1 [5, 6, 26]. Suppose the characteristic polynomial is $P(\lambda) = \lambda^2 + b\lambda + c$ of the Jacobian matrix which evaluated at the steady-state. The eigenvalues of the Jacobian matrix will satisfy Eq. (2.4) in Theorem 1 if

$$b > 0, c > 0, \tag{2.5}$$

or

$$b < 0, 4c > b^2, \left|tan^{-1}\left(\frac{\sqrt{4c-b^2}}{b}\right)\right| > \frac{\alpha\pi}{2}. \tag{2.6}$$

The stability theorem on the fractional-order systems and fractional Routh-Hurwitz stability conditions are introduced to analyze the stability of the model. The fractional Routh-Hurwitz stability conditions is specifically introduced for the eigenvalues of the Jacobian matrix that obtained in quadratic form. The proof of this proposition is shown in Appendix.

2.4. Hopf bifurcation analysis of fractional-order system

Bifurcation can be defined as any sudden change that occurs while a parameter value is varied in the differential equation system and it has a significant influence on the solution [27]. An unstable steady-state may becomes stable and vice versa. A slight changes in the parameter value may change the system's stability. Despite the steady-state point and the eigenvalues of the system of fractional-order are similar as the system of integer-order, the discriminant method used for the stability of the steady-state point is different. Accordingly, the Hopf bifurcation condition in the fractional-order system is slightly different as compared with the integer-order system.

2.4.1. Hopf bifurcation analysis of fractional order α

Fractional order α can be selected as the bifurcation parameter in a fractional-order system, but this is not allowed in an integer-order system. The existence of Hopf bifurcation can be stated as in Theorem 2.

Theorem 2 [28]. Assume α^* as the critical value of the fractional-order. When bifurcation parameter α passes over critical value α^*, which is $\alpha^* \in (0, 1)$, Hopf bifurcation occurs at the steady-state point if the following conditions are satisfied

(i) The characteristic equation of chemostat system has a pair of complex conjugate roots, $\lambda_{1,2} = p \pm iq$, while the other eigenvalues are negative real roots.

(ii) Critical value $m(\alpha^*) = \frac{\alpha^*\pi}{2} - min|arg(\lambda)| = 0$.

(iii) $\frac{dm(\alpha)}{d\alpha}|_{\alpha=\alpha^*} \neq 0$ (condition of transversality).

Proof. Condition (i) is not easy to obtain due to the selected parameter's value. However, this condition can be managed under some confined conditions. In fact, the washout steady-state solution of the chemostat model has two negative real roots. The remaining two roots depend on the characteristic of the polynomial from the no-washout steady-state solution.

Condition (ii) can be satisfied with the existence of critical value α^* and when $arg(\lambda)$ is equivalent to $arctan\left(\frac{q}{p}\right)$. Thus, the solution of critical value $m(\alpha^*)$ can be written as

$$\alpha^* = \frac{\alpha^*\pi}{2} - arctan\left(\frac{q}{p}\right) = 0, \alpha^* \in (0, 1). \tag{2.7}$$

The integer system required $p = 0$ for the bifurcation's operating condition. For the fractional-order system, the operating condition of the system will change into $m(\alpha^*) = \frac{\alpha^*\pi}{2} - min|arg(x)| = 0$. For condition (iii), the condition of $m(\alpha)$ changes when bifurcation parameter α passes over critical value α^*. For example, the steady-state point is asymptotically stable for $0 < \alpha < \alpha^*$ and unstable when $\alpha < \alpha^* < 1$. Thus, Hopf bifurcation exists at $\alpha = \alpha^*$.

2.4.2. Hopf bifurcation analysis of parameters value

In studying the dynamic process of chemostat, the parameters such as Q, S_0, μ, k, γ and β are usually used as the bifurcation parameter since these parameters have significant effects on the dynamic process of the system of fractional-order and integer-order. Fractional-order α is considered fixed and the initial substrate concentration S_0 is studied as the control parameter. The existence of the Hopf bifurcation can be stated as in Theorem 3.

Theorem 3 [28]. Assume S_0^* as the critical value of the fractional-order. When bifurcation parameter S_0 passes over critical value S_0^* , Hopf bifurcation occurs at the steady-state point if the following conditions are satisfied

(i) The characteristic equation of chemostat system has a pair of complex conjugate roots, $\lambda_{1,2} = p(S_0) \pm iq(S_0)$, while the other eigenvalues are negative real roots.

(ii) Critical value $m\left(S_0^*\right) = \frac{\alpha\pi}{2} - min|arg\left(\lambda\left(S_0^*\right)\right)| = 0.$

(iii) $\frac{dm\left(S_0^*\right)}{d\left(S_0^*\right)}|_{S_0=S_0^*} \neq 0$ (condition of transversality).

Proof. This theorem can be proved in the same way as Theorem 2. Therefore, condition (i) can be guaranteed. Condition (ii) can be satisfied with the existence of critical value S_0^* and when $arg\left[\lambda\left(S_0^*\right)\right]$ is equivalent to $arctan\left[\frac{q\left(S_0^*\right)}{p\left(S_0^*\right)}\right]$. Thus, the solution of critical value $m\left(S_0^*\right)$ can be written as

$$S_0^* = \frac{\alpha\pi}{2} - arctan\left(\frac{q\left(S_0^*\right)}{p\left(S_0^*\right)}\right) = 0. \tag{2.8}$$

For condition (iii), the condition of $m\left(S_0^*\right)$ changes when bifurcation parameter S_0 passes over critical value S_0^*. For example, the steady-state point is asymptotically stable when $0 < S_0 < S_0^*$ and unstable when $S_0 < S_0^* < 1$. Thus, Hopf bifurcation exists at $S_0 = S_0^*$ [28].

Firstly, determine the steady-states, Jacobian matrix and eigenvalues of the fractional-order chemostat model. The stability properties of the fractional-order chemostat model were estimated by using the stability and bifurcation analyses with FDEs by referring to Theorem 1 and Proposition 1. Then, determine the bifurcation point of fractional-order by referring to Theorem 2 and determine the bifurcation point of parameter values by referring to Theorem 3. Next, plot the phase portrait of fractional-order chemostat model by using Adam-types predictor-corrector method to study the dynamic behaviour of the system. Figure 1 depicts the flowchart of this research. This flowchart can be applied to all problems with suitable parameter values.

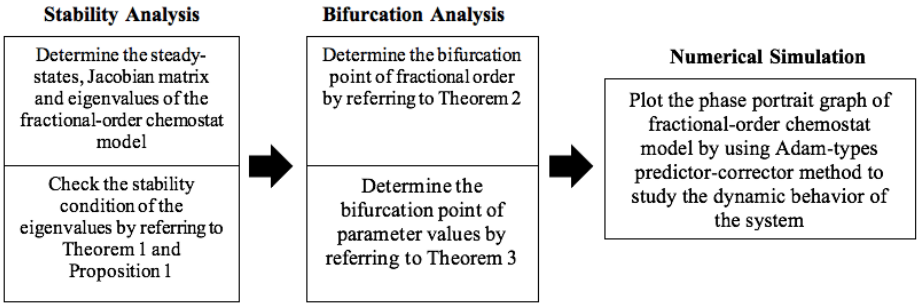

Figure 1. Mathematical analysis of fractional-order chemostat model.

3. Results and Discussion

3.1. Fractional-order chemostat model

An integer-order chemostat model that considered a variable yield coefficient and the Monod growth model from [1] is studied in this section. The chemostat system can be written as

$$\begin{aligned} \frac{dS}{dt} &= Q(S_0 - S) - \frac{\mu S X}{(k+S)(\gamma+\beta S)}, \\ \frac{dX}{dt} &= Q(-X) + \frac{\mu S X}{k+S}, \end{aligned} \tag{3.1}$$

with the initial value of $X_0 = 0$, where the sterile feed case was assumed. The integer-order chemostat system of Eq. (3.1) is extended to the fractional-order differential equation

$$\begin{aligned} \frac{d^\alpha S}{dt^\alpha} &= Q(S_0 - S) - \frac{\mu S X}{(k+S)(\gamma+\beta S)}, \\ \frac{d^\alpha X}{dt^\alpha} &= Q(-X) + \frac{\mu S X}{k+S}. \end{aligned} \tag{3.2}$$

Let Eq. (3.2) equal to zero in order to find the steady-state solutions

$$Q(S_0 - S) - \frac{\mu S X}{(k+S)(\gamma+\beta S)} = 0, \tag{3.3}$$

$$Q(-X) + \frac{\mu S X}{k+S} = 0. \tag{3.4}$$

By solving Eq. (3.4), the following solutions are obtained

$$S^* = \frac{kQ}{\mu - Q}, \tag{3.5}$$

$$X^* = 0. \tag{3.6}$$

From Eq. (3.3), if $X^* = 0$, then $S^* = S_0$. If $S^* = \frac{kQ}{\mu - Q}$, then

$$X^* = \frac{(kQ + QS_0 - S_0\mu)(-Q\gamma + kQ\beta + \gamma\mu)}{(\mu - Q)^2}. \tag{3.7}$$

Hence, the solutions of steady-state for the chemostat model are

(i) Washout:

$$(S_0^*, X_0^*) = (S_0, 0). \tag{3.8}$$

(ii) No Washout:

$$(S_1^*, X_1^*) = (\rho, (S_0 - \rho)(\gamma + \beta\rho)), \tag{3.9}$$

where

$$\rho = \frac{kQ}{\mu - Q}.$$

The steady-state solutions are physically meaningful if their components are positive. Therefore, $S_0 > 0$ for the washout steady-state solution exists by biological meaning. The no-washout steady-state solution will only exist when $0 < \rho < S_0$. The Jacobian matrix of no washout steady-state as in Eq. (3.10) can be used to investigate the stability properties of the fractional-order chemostat model.

$$J = \begin{bmatrix} -Q + \frac{X(-k\gamma + S^2\beta)\mu}{(k+S)^2(\gamma+S\beta)^2} & \frac{S\mu}{(k+S)(\gamma+S\beta)} \\ \frac{kX\mu}{(k+S)^2} & -Q + \frac{S\mu}{k+S} \end{bmatrix}. \tag{3.10}$$

3.2. Stability of washout and no-washout steady-state solution

The solution of steady-state in Equation (3.8) represents the washout situation, where the cell mass is wholly removed from the reactor and where the substrate concentration is at the same stock as in the beginning. This state must always be unstable in order to ensure that the cell mass is able to grow in the chemostat. This is because the cell mass will be continuously removed from the chemostat if the washout steady-state is stable. The Jacobian matrix for the washout steady-state solution can be written as

$$J = \begin{bmatrix} -Q & -\frac{S_0\mu}{(k+S_0)(\gamma+S_0\beta)} \\ 0 & -Q + \frac{S_0\mu}{k+S_0} \end{bmatrix}. \tag{3.11}$$

The eigenvalues of this matrix are

$$\lambda_1 = -Q, \tag{3.12}$$

$$\lambda_2 = \frac{-kQ - QS_0 + S_0\mu}{k + S_0}. \tag{3.13}$$

The eigenvalues in Eq. (3.12) and Eq. (3.13) are real. The washout steady-state solution is stable if $Q > 0$ and $\rho > S_0$ where $\rho = \frac{kQ}{\mu - Q}$. The steady-state solution in Eq. (3.9) represents the no-washout situation. No-washout situation is where the cell mass is not removed and stay growth in the

chemostat.This state is important. The steady-state solution is substituted into the Jacobian matrix in Eq. (3.10) and can be written as

$$J = \begin{bmatrix} -Q + \frac{\mu(S_0-\rho)\left(\beta\rho^2-k\gamma\right)}{(k+\rho)^2(\beta\rho-\gamma)} & -\frac{\mu\rho}{(k+\rho)(\beta\rho+\gamma)} \\ \frac{k\mu(S_0-\rho)(\beta\rho-\gamma)}{(k+\rho)^2} & -Q + \frac{\mu\rho}{k+\rho} \end{bmatrix}. \tag{3.14}$$

The eigenvalues of the Jacobian matrix in terms of the characteristic polynomial are

$$P(\lambda) = \lambda^2 + b\lambda + c, \tag{3.15}$$

where

$$b = 2Q + \frac{\mu(S_0 - 2\rho)}{(k+\rho)} + \frac{\mu\rho(\rho - S_0)}{(k+\rho)^2} + \frac{\beta\mu\rho(\rho - S_0)}{(k+\rho)(\gamma+\beta\rho)}, \tag{3.16}$$

and

$$\begin{aligned} c =& Q^2 + \frac{Q\mu(S_0 - 2\rho)}{(k+\rho)} + \frac{(\mu\rho - S_0\mu)(\mu\rho - Q\rho)}{(k+\rho)^2} + \frac{\mu^2\rho^2(S_0 - \rho)}{(k+\rho)^3} \\ &- \frac{Q\beta\mu\rho(S_0 - \rho)}{(k+\rho)(\gamma+\beta\rho)} + \frac{(S_0\mu - \mu\rho)\left(\mu\rho\gamma + 2\mu\beta\rho^2\right)}{(k+\rho)^2(\gamma+\beta\rho)} \\ &+ \frac{(\mu\rho - S_0\mu)\left(\mu\rho^2\gamma + \mu\beta\rho^3\right)}{(k+\rho)^3(\gamma+\beta\rho)}. \end{aligned} \tag{3.17}$$

The eigenvalues of the no-washout steady-state solution were evaluated with Routh-Hurwitz condition in Proposition 1. Based on the eigenvalues in Eq. (3.15) and by referring to the study by [5], the eigenvalues' condition can be simplified as the following two cases

(i) If $b > 0$ or equivalent to $\frac{\gamma}{\beta} > P_1$, the no-washout steady-state solution of the system in Eq. (3.2) is asymptotically stable. P_1 can be written as

$$P_1 = -\frac{\mu\rho(\rho - S_0)}{2Q(k+\rho)} - \frac{\rho(\rho - S_0)}{(S_0 - \rho)} - \frac{(k+\rho)}{\mu\rho(\rho - S_0)} - \rho, \tag{3.18}$$

(ii) If $b < 0$ or equivalent to $\frac{\gamma}{\beta} < P_1$ and $tan^{-1}\left(\frac{\sqrt{4c-b^2}}{b}\right) > \frac{\alpha\pi}{2}$, the no-washout steady-state solution of the system in Eq. (3.2) is asymptotically stable. The condition of $tan^{-1}\left(\frac{\sqrt{4c-b^2}}{b}\right) > \frac{\alpha\pi}{2}$ is also equivalent to $4cos^2\left(\frac{\alpha\pi}{2}\right)c > b^2$, which can be simplified as $\frac{\gamma}{\beta} > P_2$. Then, this case can be concluded and written as $P_2 < \frac{\gamma}{\beta} < P_1$ where

$$P_2 = \frac{\mu\rho(\rho - S_0)}{2cos\left(\frac{\alpha\pi}{2}\right)\sqrt{c}(k+\rho)} - \frac{\mu\rho(\rho - S_0)}{2Q(k+\rho)} - \frac{\rho(\rho - S_0)}{(S_0 - \rho)} - k - 2\rho. \tag{3.19}$$

Then, if $P_2 < \frac{\gamma}{\beta} < P_1$, the no-washout steady-state solution of the system in Eq. (3.2) is asymptotically stable.

The parameter values of the fractional-order chemostat model are provided in Table 1. The initial substrate concentration, S_0 and ρ were assumed as non-negative values to ensure that the steady-state solutions were physically meaningful. The stability diagram of the steady-state solutions is plotted in Figure 2.

Table 1. Parameter values.

Parameters	Description	Values	Units
k	Saturation constant	1.75	gl^{-1}
Q	Dilution rate	0.02	l^2gr^{-1}
μ	Maximum growth rate	0.3	h^{-1}
γ	Constant in yield coefficient	0.01	–
β	Constant in yield coefficient	5.25	lg^{-1}
S_0	Input concentration of substrate	1	gl^{-1}

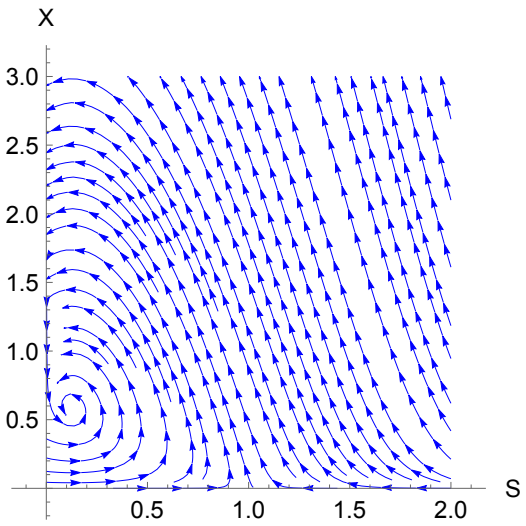

Figure 2. Stability diagram of the steady-state solutions when $\alpha = 1$.

The washout steady-state solution is stable if $Q > 0$ and $\rho > S_0$. From Figure 2, it shows that the unstable solution of washout steady-state, as the eigenvalues did not fulfil the condition of $\rho > S_0$. By choosing the appropriate parameter values, the unstable washout steady-state solution could ensure that the washout condition does not occur in the chemostat. Meanwhile, the solution of no-washout steady-state is stable.

3.3. Hopf bifurcation analysis of the order of fractional-order system

The steady-state solutions of the fractional-order chemostat model for the parameter values given in Table 1 are

(i) Washout:

$$(S_0^*, X_0^*) = (1, 0)\,, \tag{3.20}$$

(ii) No Washout:

$$(S_1^*, X_1^*) = \left(\frac{1}{8}, \frac{3731}{6400}\right). \tag{3.21}$$

The eigenvalues obtained from the washout steady-state solution are

$$\lambda_1 = -\frac{1}{50}, \tag{3.22}$$

$$\lambda_2 = -\frac{49}{550}, \tag{3.23}$$

and the eigenvalues from the no-washout steady-state solution are

$$\lambda_1 = \frac{-2552 + \sqrt{411098126i}}{399750}, \tag{3.24}$$

$$\lambda_2 = \frac{-2552 - \sqrt{411098126i}}{399750}, \tag{3.25}$$

Based on Eq. (3.22) to Eq. (3.25), these satisfied the first condition of Hopf bifurcation in Theorem 2. There exists a pair of complex conjugate roots and the other eigenvalues are negative real roots. The transversality condition as the third condition is also satisfied. The eigenvalues of the washout steady-state solution based on the chemostat system is not imaginary, and so there is no existence of Hopf bifurcation in the washout steady-state solution. According to Theorem 2, the critical value of the fractional-order as stated in the second condition can be obtained as

$$m(\alpha^*) = \frac{\alpha^*\pi}{2} - min|arg(\lambda)| = 0, \tag{3.26}$$

$$\alpha^* = \frac{2}{\pi} min|arg(\lambda)|, \tag{3.27}$$

where

$$arg(\lambda) = arctan\left(\frac{q}{p}\right), \tag{3.28}$$

$$\alpha^* = \frac{2}{\pi} arctan\left(\frac{q}{p}\right) = \frac{2}{\pi} arctan\left(\frac{\frac{\sqrt{411098126}}{399750}}{\frac{2552}{399750}}\right) = 0.9202904711 \approx 0.9. \tag{3.29}$$

Value of p and q are obtained from Eq. (3.24) and Eq. (3.25) by assuming parameter value in Table 1. Hence, when $\alpha^* = 0.9$, the chemostat system in Eq. (3.2) shows Hopf bifurcation, at which the system stability would be altered.

Figure 3 is plotted to determine the dynamic behaviour at the Hopf bifurcation point. The phase portrait diagrams of cell mass concentration against substrate concentration are plotted for values of order of the fractional is $\alpha = 0.9$.

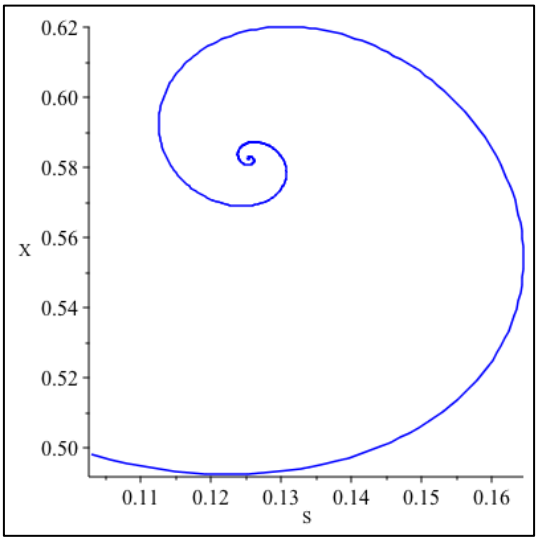

Figure 3. Phase portrait plot of fractional-order chemostat system with $\alpha = 0.9$.

The running state of the fractional-order chemostat system when fractional order α at the Hopf bifurcation point is shown. The fractional-order chemostat system changed its stability once Hopf bifurcation occurred. Therefore, we conjecture that the system of fractional-order chemostat may be lost or gain its stability when the fractional order α is less than the Hopf bifurcation point, or $\alpha < 0.9$ or otherwise. This shows that increasing or decreasing the value of α may destabilise the stable state of the chemostat system. Therefore, these results show that the running state of the fractional-order chemostat system is affected by the value of α.

3.4. Hopf bifurcation analysis of initial concentration of substrate

The initial concentration of the substrate, S_0, was chosen as the control parameter, while fractional order α was fixed. The solutions of steady-state of the fractional-order chemostat model with S_0 as the control parameter are

(i) Washout:

$$(S_0^*, X_0^*) = (S_0, 0)\,, \tag{3.30}$$

(ii) No Washout:

$$(S_1^*, X_1^*) = \left(\frac{1}{8}, \frac{533(-1 + 8S_0)}{6400}\right). \tag{3.31}$$

The eigenvalues obtained from the washout steady-state solution are

$$\lambda_1 = -\frac{1}{50}, \tag{3.32}$$

$$\lambda_2 = -\frac{7(1-8S_0)}{50(-7-4S_0}, \tag{3.33}$$

and the eigenvalues from the no-washout steady-state solution are

$$\lambda_1 = -4204 + 1652S_0 + \frac{\sqrt{2}\sqrt{1364552S_0^2 - 245579768S_0 + 38666153}}{399750}i, \tag{3.34}$$

$$\lambda_2 = -4204 + 1652S_0 - \frac{\sqrt{2}\sqrt{1364552S_0^2 - 245579768S_0 + 38666153}}{399750}i. \tag{3.35}$$

These satisfied the first condition of Hopf bifurcation in Theorem 3. There exist a pair of complex conjugate roots in terms of S_0, and the other eigenvalues were negative real roots in terms of S_0. The transversality condition as the third condition is also satisfied. According to Theorem 3, the critical value of the fractional order as stated in the second condition can be obtained as follows

$$m(S_0^*) = \frac{\alpha^*\pi}{2} - min|arg(\lambda)| = 0. \tag{3.36}$$

By referring to the study by [18], Eq. (3.37) can also be calculated as

$$\frac{q'\left(S_0^*\right)p\left(S_0^*\right) - q\left(S_0^*\right)p'\left(S_0^*\right)}{q^2\left(S_0^*\right) + p^2\left(S_0^*\right)} \neq 0. \tag{3.37}$$

From the calculations, the critical value of the initial concentration of the substrate is $S_0 = 2.54$. When $S_0 = 2.54$, the chemostat system shows Hopf bifurcation, at which the stability of the system would be altered.

Figure 4 presents the phase portrait diagrams of concentration of cell mass against concentration of substrate when $\alpha = 1$ for different values of the initial concentration of the substrate, which are $S_0 = 2$, $S_0 = 2.54$ and $S_0 = 3.5$.

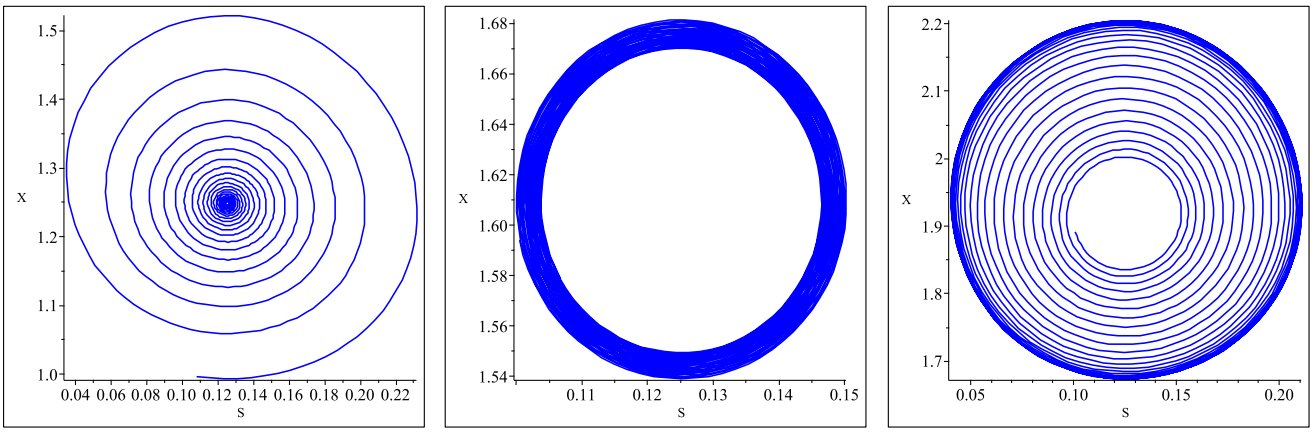

(a) (b) (c)

Figure 4. Phase portrait plot of chemostat system with $\alpha = 1$ (a) $S_0 = 2$ (b) $S_0 = 2.54$ and (c) $S_0 = 3.5$.

The change in the running state when the value of the initial substrate concentration passes through the Hopf bifurcation point is shown. The stability of the fractional-order chemostat system changed once Hopf bifurcation occurred. In Figure 3(a), the fractional-order chemostat system is in a stable state when the initial substrate concentration value is less than the Hopf bifurcation point, or $S_0 < 2.54$. Meanwhile, when the value of the initial substrate concentration passes through the Hopf bifurcation point, or $S_0 \geq 2.54$, the fractional-order chemostat system lost its stability. This shows that increasing the value of the initial substrate concentration may destabilise the stable state of the chemostat system. These results show that the running state of the fractional-order chemostat system is affected by the value of the initial substrate concentration. In real-life application, the value of the initial substrate should remain at $S_0 \geq 2.54$ to ensure that the chemostat system is at the unstable state. This is because the unstable state is suitable for the production of cell mass [1]. Unstable state means the system always move away after small disturbance, so the system must be at the unstable state because there will be a change in amount of cell mass production.

Figure 5 depicts the phase portrait diagrams of cell mass concentration against substrate concentration when $\alpha = 0.9$ for different values of the initial concentration of the substrate, which are $S_0 = 2$, $S_0 = 2.54$ and $S_0 = 3.5$.

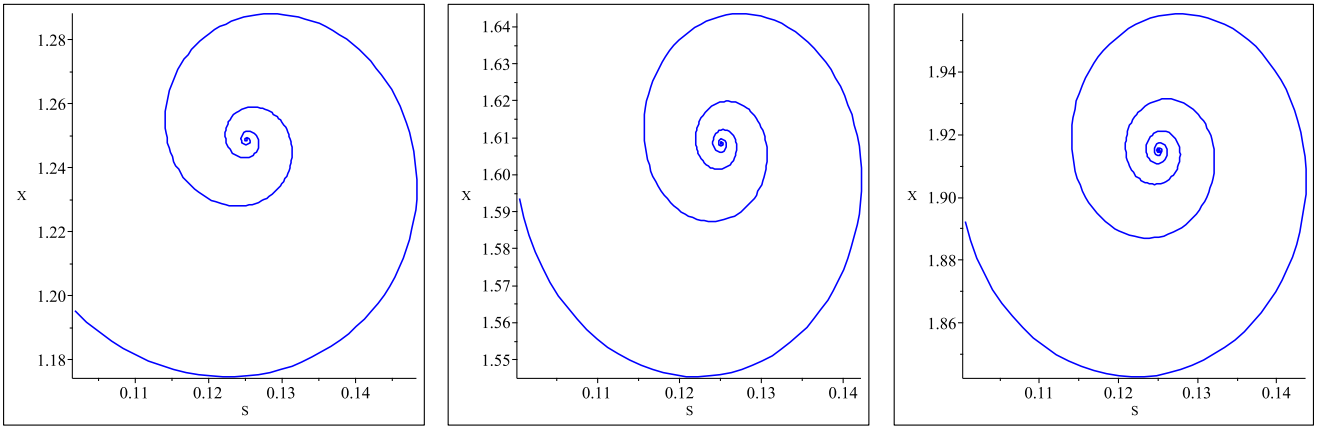

(a) (b) (c)

Figure 5. Phase portrait plot of chemostat system with $\alpha = 0.9$ (a) $S_0 = 2$ (b) $S_0 = 2.54$ and (c) $S_0 = 3.5$.

The Hopf bifurcation points of system of fractional-order chemostat and system of integer-order chemostat are different. Figure 4 shows the fractional-order chemostat system at a stable state for all values of the initial substrate concentration when $\alpha = 0.9$. The chemostat system destabilised the stable state when the initial substrate concentration value is $S_0 \geq 2.54$, as shown in Figure 3(b) and Figure 3(c). This shows that the dynamic behaviour of the fractional-order chemostat system is different compared with the integer-order chemostat system. In actual application, the value of the initial substrate should remain at $S_0 \geq 2.54$ to ensure that the chemostat system can be well controlled in order to be suitable for cell mass production.

4. Conclusions

The stability analysis of the fractional-order chemostat model was conducted based on the stability theory of FDEs. The integer-order chemostat model was extended to the FDEs. There are two steady-state solutions obtained, which are washout and no-washout steady-state solutions. The Hopf bifurcation of the order of α occured at the solutions of steady-state when the Hopf bifurcation conditions is fulfilled. The results show that the increasing or decreasing the value of α may stabilise the unstable state of the chemostat system. Therefore, the running state of the fractional-order chemostat system is affected by the value of α. The Hopf bifurcation of the initial concentration of the substrate, S_0, also occurred when the Hopf bifurcation condition is fulfilled. As the evidence from the phase portrait plots, increase the value of the initial substrate concentration may destabilise the stable state of the chemostat system. The value of the initial substrate should remain at $S_0 \geq 2.54$ to ensure that the chemostat system is at the unstable state since the unstable state is suitable for the production of cell mass. These dynamical analyses are important to provide suitable values of the fractional-order and the parameters in order to ensure the controllability and stability of the chemostat to suit the actual chemostat environment.

Acknowledgments

We would like to express our gratitude sincere for the financial support by the Universiti Tun Hussein Onn Malaysia through the grant H426.

Conflict of interest

No conflict of interest is declared by the authors.

References

1. Nelson MI, Sidhu HS (2005) Analysis of a chemostat model with variable yield coefficient. *J Math Chem* 38: 605–615.
2. Harmand J, Lobry C, Rapaport A, et al. (2017) The chemostat: Mathematical theory of microorganism cultures, John Wiley & Sons.
3. Elettreby MF, Al-Raezah AA, Nabil T (2017) Fractional-order model of two-prey one-predator system. *Math Probl Eng* 2017: 6714538.
4. Cui X, Yu Y, Wang H, et al. (2016) Dynamical analysis of memristor-based fractional-order neural networks with time delay. *Mod Phys Lett B* 30: 1650271.
5. Zeinadini M, Namjoo M (2016) A numerical method for discrete fractional-order chemostat model derived from nonstandard numerical scheme. *B Iran Math Soc* 43: 1165–1182.
6. Zeinadini M, Namjoo M (2017) Approximation of fractional-order chemostat model with nonstandard finite difference scheme. *Hacet J Math Stat* 46: 469–482.
7. Garrappa R (2018) Numerical solution of fractional differential equations: A survey and a software tutorial. *Mathematics* 6: 16.

8. Islam MR, Peace A, Medina D, et al. (2020) Integer versus fractional order seir deterministic and stochastic models of measles. *Int J Env Res Pub He* 17: 2014.
9. Nelson MI, Sidhu HS (2009) Analysis of a chemostat model with variable yield coefficient: tessier kinetics. *J Math Chem* 46: 303–321.
10. Ahmed E, Hashish A, Rihan FA (2012) On fractional order cancer model. *J Fract Calc Appl Anal* 3: 1–6.
11. Sidhu HS, Nelson MI, Balakrishnan E (2015) An analysis of a standard reactor cascade and a step-feed reactor cascade for biological processes described by monod kinetics. *Chem Prod Process Model* 10: 27–37.
12. Alqahtani RT, Nelson MI, Worthy AL (2015) Analysis of a chemostat model with variable yield coefficient and substrate inhibition: contois growth kinetics. *Chem Eng Commun* 202: 332–344.
13. Ezz-Eldien SS (2018) On solving fractional logistic population models with applications. *Comput Appl Math* 37: 6392–6409.
14. D'Ovidio M, Loreti P, Ahrabi SS (2018) Modified fractional logistic equation. *Physica A* 505: 818–824.
15. Khater M, Attia RAM, Lu D (2019) Modified auxiliary equation method versus three nonlinear fractional biological models in present explicit wave solutions. *Math Comput Appl* 24: 1.
16. Sayari S, El Hajji M (2019) How the fractional-order improve and extend the well-known competitive exclusion principle in the chemostat model with n species competing for a single resource? *Asian Res J Math* 12: 1–12.
17. Isah A, Phang C (2018) Operational matrix based on Genocchi polynomials for solution of delay differential equations. *J Ain Sham Eng* 9: 2123–2128.
18. Li X, Wu R (2014) Hopf bifurcation analysis of a new commensurate fractional-order hyperchaotic system. *Nonlinear Dynam* 78: 279–288.
19. De Oliveira EC, Tenreiro Machado JA (2014) A review of definitions for fractional derivatives and integral. *Math Probl Eng* 2014: 238459.
20. Diethelm K, Freed AD (1999) On the solution of nonlinear fractional-order differential equations used in the modeling of viscoplasticity, *Scientific Computing in Chemical Engineering II*, Berlin: Springer, 217–224.
21. Toh YT, Phang C, Loh JR (2019) New predictor-corrector scheme for solving nonlinear differential equations with Caputo-Fabrizio operator. *Math Method Appl Sci* 42: 175–185.
22. Diethelm K, Ford NJ, Freed AD (2002) A predictor-corrector approach for the numerical solution of fractional differential equations. *Nonlinear Dynam* 29: 3–22.
23. Ghrist ML, Fornberg B, Reeger JA (2015) Stability ordinates of Adams predictor-corrector methods. *BIT Numer Math* 55: 733–750.
24. Matignon D (1996) Stability results for fractional differential equations with applications to control processing. *Comput Eng Syst Appl* 2: 963–968.
25. Vinagre BM, Monje CA, Calderón AJ, et al. (2007) Fractional PID controllers for industry application. A brief introduction. *J Vib Control* 13: 1419–1429.

26. Ahmed E, El-Sayed AMA, El-Saka HAA (2006) On some Routh–Hurwitz conditions for fractional order differential equations and their applications in Lorenz, Rössler, Chua and Chen systems. *Physics Letters A* 358: 1–4.

27. Karaaslanli CC (2012) Bifurcation analysis and its applications, In: Andriychuk, M., Numerical simulation from theory to industry, Croatia: INTECH open access publisher.

28. Ma J, Ren W (2016) Complexity and Hopf bifurcation analysis on a kind of fractional-order IS-LM macroeconomic system. *Int J Bifurcat Chaos* 26: 1650181.

AIMS Press